

Received June 17, 2020, accepted August 27, 2020, date of publication September 4, 2020, date of current version September 18, 2020.

Digital Object Identifier 10.1109/ACCESS.2020.3021801

# Quantitatively Isolating Extratropical Atmospheric Impact on the Tropical Pacific Interannual Variability in Coupled Climate Model

JINGZHE SUN<sup>1,2,3</sup>, ZHENGYU LIU<sup>3</sup>, FEIYU LU<sup>4,5</sup>, WEIMIN ZHANG<sup>6,7</sup>,  
YUCHU ZHAO<sup>3,8</sup>, AND SHAOQING ZHANG<sup>9,10,11,12</sup>

<sup>1</sup>College of Computer, National University of Defense Technology, Changsha 410073, China

<sup>2</sup>Open Studio for Ocean-Climate-Isotope Modeling, Qingdao National Laboratory for Marine Science and Technology, Qingdao 266000, China

<sup>3</sup>Atmospheric Science Program, Department of Geography, The Ohio State University, Columbus, OH 43210, USA

<sup>4</sup>Atmospheric and Oceanic Sciences Program, Princeton University, Princeton, NJ 08544, USA

<sup>5</sup>NOAA/Geophysical Fluid Dynamics Laboratory, Princeton, NJ 08540, USA

<sup>6</sup>College of Meteorology and Oceanography, National University of Defense Technology, Changsha 410073, China

<sup>7</sup>Laboratory of Software Engineering for Complex Systems, National University of Defense Technology, Changsha 410073, China

<sup>8</sup>Department of Atmospheric and Oceanic Sciences, Peking University, Beijing 100871, China

<sup>9</sup>Key Laboratory of Physical Oceanography, College of Oceanic and Atmospheric Sciences, Ocean University of China, Qingdao 266100, China

<sup>10</sup>Institute for Advanced Ocean Study, Ocean University of China, Qingdao 266100, China

<sup>11</sup>Function Laboratory for Ocean Dynamics and Climate, Qingdao National Laboratory for Marine Science and Technology, Qingdao 266000, China

<sup>12</sup>International Laboratory for High-Resolution Earth System Prediction, Qingdao 266000, China

Corresponding author: Jingzhe Sun (sunjingzhe13@nudt.edu.cn)

This work was supported in part by the National Key Research and Development Programs of China under Grant 2018YFC1406202 and Grant 2018YFC1506704; in part by the U.S. NSF under Grant AGS-1656907; in part by the Chinese MOST under Grant 2017YFA0603801; and in part by the Chinese NSF under Grant 41775100, Grant 41830964, and Grant 41605070.

**ABSTRACT** Recent studies have demonstrated a significant control of extratropical atmospheric forcing on the tropical Pacific interannual variability. However, it remains unclear how the extratropical atmospheric signal is transferred equatorward via potential pathways. Here aided by regional coupled data assimilation and partial restoring techniques, the extratropical atmospheric impact on the tropical Pacific interannual variability is quantitatively isolated into atmospheric, oceanic and coupled ocean-atmosphere teleconnections at different latitudes in a coupled general circulation model. Results show that poleward of 20°, the atmospheric pathway dominates the extratropical impact on the tropical Pacific, accounting for 90% of the total contribution. Towards the equator, less contribution is attributed to the atmospheric pathway, while more to the coupled ocean-atmosphere teleconnections and the oceanic pathway. Poleward of 10°, contribution from the atmosphere rapidly decreases to 46%, while impact from coupled interactions significantly increases to 46% and that from the ocean slightly increases to 8%. Composite analyses show that coupled interactions between 10° and 20° significantly impact the ENSO (El Niño-Southern Oscillation) onset by modulating the Pacific meridional mode and the preconditioning of equatorial Pacific heat content.

**INDEX TERMS** Coupled climate model, coupled data assimilation, extratropical impact, partial restoring, tropical Pacific interannual variability.

## I. INTRODUCTION

Meridional teleconnections responsible for the extratropical impact on tropical variability remain to be further explored. In this study, teleconnection generally indicates the linkage of climate variabilities among components of the Earth system over great distances [1]. Boosted by the need to understand

The associate editor coordinating the review of this manuscript and approving it for publication was Haiyong Zheng .

Pacific decadal variability (PDV) [2], [3], great interest has been devoted to the role of extratropics-tropics connections in the climate system. The tropical impact on the extratropical climate has been extensively studied due to the prominent importance of the El Niño-Southern Oscillation (ENSO) in the Earth system, while the extratropical impact on the tropics still faces many unanswered questions. Studies have demonstrated that the tropical impact on the extratropical climate is mainly carried out via the atmospheric bridge [4]–[6].

The extratropical influence on tropical variability, however, may be attributed to three pathways: atmospheric teleconnections, oceanic teleconnections, and coupled ocean-atmosphere teleconnections (hereafter “surface coupling”).

The equatorward extratropical teleconnections can be accomplished through the atmosphere on regional to global scales [1]. On regional to basin scales, the atmospheric response to the sea surface temperature (SST) anomaly (SSTA) variations in the Kuroshio extension region can extend into the tropics [7], [8]. Large-scale disturbances in the middle latitudes may have a significant impact on equatorial regions through the westerly duct [9]. In addition, changes in sea ice may also have the potential to impact the tropical climate via the atmosphere [10], [11]. The extratropical influence on the tropics can also take place via oceanic teleconnections. At centennial or longer timescales, equatorward ventilation plays an important role in basin-scale climate change [12]–[15]. At interdecadal or shorter timescales, the first-mode baroclinic Rossby wave tends to have a greater influence than ventilation. At the western boundary, the coastal Kelvin wave is critical to the ocean circulation adjustments [16], [17] and may also facilitate the influence of extratropical decadal variability on the tropical Pacific and Atlantic [18], [19]. Equatorward thermocline subduction from the subtropics can impact the tropical Pacific through the western boundary and interior exchange windows [20], [21]. Furthermore, the coupling interactions at the air-sea interface serve as another important type of teleconnection to transmit the extratropical impact into the tropics. Different from the two pathways discussed above, surface coupling critically depends on the coupling interactions between the atmosphere and the ocean. A fast equatorward coupled teleconnection was proposed by Liu and Xie [22], which depends on the wind-evaporation-SST (WES) feedback and can carry the subtropical signal to deep tropics in months. ENSO variability could be generated by extratropical atmospheric variability via the seasonal footprinting mechanism (SFM) [23]–[25] or the North Pacific meridional mode (NPMM) [26], [27] from the North Pacific and through the South Pacific meridional mode (SPMM) [28] from the South Pacific. The North and South Pacific extratropical atmospheric variability also exhibits a joint impact on the onset of ENSO [29]. A similar mechanism is also recognized in the Atlantic [26], [30]. This coupled teleconnection further helps to understand the impact of the North Atlantic Oscillation on the tropical Atlantic decadal oscillation [31] and the equatorward penetration of North Pacific decadal variability [32], [33].

As a pilot study, the main goal here is to isolate and quantitatively assess the impact of the extratropical atmosphere on the interannual variability of tropical Pacific via three pathways. Previous studies tend to focus on understanding the extratropics-tropics connections from qualitative perspective, which usually explored the teleconnections separately in the atmosphere, ocean, or ocean-atmosphere interface.

Few studies have quantitatively assessed the extratropical impact on the tropics with all three types of teleconnections. Lu *et al.* [34] (hereafter “L17”) studied the control of the extratropical atmosphere on tropical Pacific variability in a coupled general circulation model (CGCM). However, impact of three pathways in the coupled model were mixed together. The individual contribution of each pathway remains unclear. In this study, a series of CGCM experiments are designed with the aid of two modeling “surgery” techniques: regional coupled data assimilation (RCDA) and partial restoring (PR). The relative contribution of each type of teleconnections at different latitudes in transferring extratropical variability into the tropical Pacific is systematically and quantitatively studied. To the best of our knowledge, this is the first study to quantitatively isolate the extratropical impact on the tropics into three types of teleconnections in a CGCM. This paper is organized as follows. Section 2 describes the CGCM we used in this study, two modeling “surgery” strategies, and the design of experiments. The results are reported in section 3. Section 4 discusses the results and summarizes the paper.

## II. DATA AND METHOD

### A. MODEL

The Fast Ocean Atmosphere Model (FOAM) [35] is a fully coupled climate model that has been used in several previous studies on coupled data assimilation (CDA) [36]–[38] and climate dynamics [34], [39], [40]. The atmosphere component is a spectral model with an R15 horizontal resolution and 18 vertical levels. The ocean component is based on the Modular Ocean Model with a  $2.8^\circ \times 1.4^\circ$  horizontal resolution and 24 z-coordinate levels. The land surface and sea ice models are also included. FOAM is able to capture most major features of the observed climatology and climate variability as in some state-of-the-art CGCMs. The CDA system in FOAM, which consists of the atmosphere DA (ADA) and the ocean DA (ODA), is based on the ensemble adjustment Kalman filter (EAKF) [41]–[43]. Schemes for localization and covariance inflation are both included. A detailed description of the CDA system in FOAM can be found in Lu *et al.* [38].

### B. RCDA AND PR

The RCDA method is used to limit the assimilation to desired model components and domains [34], [39]. In the assimilation regions, the model ensemble is continuously “nudged” towards the observations through the EAKF approach. Then the ensemble-mean model response in regions without assimilation can be analyzed when the selected assimilation component is activated in only limited regions (e.g., tropical response to observed extratropical atmosphere). While the use of a coupled model allows the fully coupled dynamics over the globe. A prominent advantage of RCDA here is to separate the extratropical signal that triggers tropical variability from the tropical

**TABLE 1.** Experiment design. Root-mean-square errors (RMSEs) and anomaly correlation coefficients (ACCs) are calculated based on the ensemble-mean SSTA in the tropical Pacific (10°S–10°N, 120°E–70°W). Confidence levels are based on a Student's t test after accounting for lag-1 autocorrelation.

Experiment	DA	DA Latitude	PR	PR Latitude	RMSE	ACC	Explained Variance (%)	Confidence Level (%)
ctrl	None	None	None	None	0.592	0.024	<1	8
adaall	ADA	All	None	None	0.142	0.968	94	>99
ada30	ADA	>30°N & <30°S	None	None	0.429	0.672	45	>99
cda30	CDA	>30°N & <30°S	None	None	0.431	0.670	45	>99
subpr20	ADA	>30°N & <30°S	subPR	20°–30°N & 20°–30°S	0.433	0.665	44	>99
colpr20	ADA	>30°N & <30°S	colPR	20°–30°N & 20°–30°S	0.446	0.639	41	>99
subpr10	ADA	>30°N & <30°S	subPR	10°–20°N & 10°–20°S	0.444	0.646	42	>99
colpr10	ADA	>30°N & <30°S	colPR	10°–20°N & 10°–20°S	0.521	0.458	21	>98

climate itself, such that the sole extratropical impact on the tropical climate can be unambiguously studied [34]. The joint usage of limited assimilation, full dynamics, and ensemble approach makes RCDA a flexible and effective method for studying teleconnections in a coupled climate system.

The PR approach is adopted to block the extratropics-tropics connections in the ocean component, thus evaluating the roles of surface coupling and oceanic teleconnections in the climate system [44]–[46]. With the PR technique, “sponge walls” are inserted into the ocean component of the coupled model at specified latitude bands across the globe. Within the sponge walls, temperature and salinity are restored towards the annual cycle climatology of the control run (without assimilation), thus cutting-off the variability connections in the meridional direction of the ocean. To further separate surface coupling from oceanic dynamic teleconnections, the PR approach will be used here in two forms: column PR (colPR) and subsurface PR (subPR). In colPR, sponge walls are inserted from the ocean surface to the bottom; thus, surface coupling and oceanic dynamic teleconnections are both cut-off in the meridional direction by colPR walls. While in subPR, restoring walls are only placed from ocean depth of 50 m downward to the bottom. Here the ocean depth of 50 m is chosen because this is a typical value of the ocean mixed layer [47] and it is also consistent with the mixed layer depth in FOAM calculated from a 200-year simulation. Thus, subPR allows us to cut-off oceanic meridional teleconnections, which critically depend on ocean dynamics, but the coupled ocean-atmosphere interactions can be reserved.

Aided by RCDA and PR methods, the extratropical impact on the tropical Pacific can be separated into three pathways. Here we will focus on the forcing role of the extratropical atmosphere on the tropical Pacific, such that the ADA component of the CDA system is activated in the extratropical atmosphere in most experiments. The sole use of ADA ensures that the extratropical atmosphere is the only source of the observational information; thus, the tropical variability can be exclusively generated by the extratropical atmospheric signal. And the use of a coupled climate model guarantees

the fully coupled dynamics both inside and outside the assimilation regions. When the subPR is further adopted into the ocean, the oceanic teleconnections are cut-off, such that only the atmospheric pathway and surface coupling can transfer the extratropical signal equatorward. Instead, if both surface coupling and the oceanic pathway are cut-off by colPR, the extratropical signal can only impact the tropics via the atmospheric pathway. As such, the extratropical impact on the tropical Pacific is separated into three pathways.

### C. EXPERIMENT DESIGN

A series of experiments are performed in this study aided by the RCDA and PR techniques (Table 1). In the ctrl experiment, neither assimilation nor restoring is turned on. The experiments with only active ADA include those with the ADA activated at all latitudes (adaall) and poleward of 30° (ada30) in both hemispheres. In the assimilation regions, the model ensemble is continuously “nudged” towards the observations. In addition to regional ADA, ODA is further activated in the same extratropical regions in the cda30 experiment. Based on the regionally activated ADA of the ada30 experiment, experiments with restoring walls further inserted into the ocean consist of those with subPR walls (subprN) and colPR walls (colprN), where the integer “N” indicates that restoring walls are inserted between latitudes N and N+10 in both hemispheres. In this study, restoring walls are placed at two different latitude belts: between 20° and 30° and between 10° and 20°.

A perfect-model framework is adopted in this study, which uses the output of a single-member run as the “truth”. This twin-experiment setup allows us to reasonably simplify the complex question in the real world and provides a reliable comparison reference in this study. Pseudo-observations are generated by adding Gaussian white noise onto the truth; thus, they are gridded data at the same grid-points as the model variables. The assimilated observations in ADA include the 1-day-mean atmosphere temperature (T) and wind components (U, V) with error scales of 0.1 K and 0.1 m/s, respectively. The available observations in ODA are 5-day-mean SST with an error scale of 0.1 K.

The frequencies for ADA and ODA are every day and every 5 days, respectively, and a timescale of 1 day is used for the PR. All experiments consist of 16 ensemble members, and the initial conditions of 16 consecutive years of the atmosphere component are used to generate the initial ensemble. All experiments are conducted for 57 years. The data assimilation and partial restoring are both activated after 2 years of spin-up and last for 55 years, and the last 55 years are used for analysis. The ensemble-mean output is calculated by averaging the monthly outputs of all 16 ensemble members. The variable anomaly is computed by subtracting the annual cycle climatology from the corresponding monthly output. Both anomaly correlation coefficient (ACC) and anomaly root-mean-square error (RMSE) are used for the analysis of results:

$$ACC = \frac{\sum_{i=1}^n (x_i - \bar{x})(y_i - \bar{y})}{\sqrt{\sum_{i=1}^n (x_i - \bar{x})^2} \sqrt{\sum_{i=1}^n (y_i - \bar{y})^2}} \quad (1)$$

$$RMSE = \sqrt{\frac{1}{n} \sum_{i=1}^n (x_i - y_i)^2} \quad (2)$$

where  $n$  is the number of months,  $x_i$  is the ensemble-mean anomaly of the  $i$ th monthly mean output from the ensemble experiments,  $y_i$  is the anomaly of the  $i$ th monthly mean output from the truth, and  $\bar{x}$  and  $\bar{y}$  are the means of  $x_i$  and  $y_i$  of all months, respectively. Consistent results are obtained using ACC and RMSE, and the presented results are mainly based on ACC. In this study, the tropical Pacific indicates the Pacific region of  $(10^{\circ}\text{S}-10^{\circ}\text{N}, 120^{\circ}\text{E}-70^{\circ}\text{W})$ , and the tropical Pacific variability represents the interannual variability of tropical Pacific SST, unless otherwise specified, to account for ENSO - the strongest interannual variability in the tropical Pacific.

### III. RESULTS

#### A. GENERAL ASSESSMENT

The extratropical atmosphere shows a significant control on the tropical Pacific variability. When no assimilation is activated across the globe, the tropical Pacific ensemble-mean SSTA of ctrl fails to reproduce the truth (Figure 1a). The use of ensemble averaging minimizes the noise from natural variability of each member. Although each member has its own variability, the ensemble-mean SSTA filters out the internal variabilities of individual members and always stays close to 0. As a result, the ACC (RMSE) of SSTA is very small (large) with almost no ( $<1\%$ ) tropical Pacific variance explained. When ADA is activated at all latitudes, the model closely follows the truth with a significant ACC of tropical Pacific SSTA as high as 0.968 at the 99% confidence level and a significantly reduced RMSE of 0.142 (Figure 1b) with almost all (94%) tropical Pacific variance explained. When the atmosphere is well constrained by observations across the globe, the underlying ocean can also be largely improved for the better boundary conditions provided by the overlying atmosphere. This also verifies the effectiveness of our ADA component in well constraining the atmosphere status. Thus ctrl and adaall represent the worst and best

extremes, respectively, that our model can achieve in this study. When the equator-side boundaries of the activated ADA move poleward to  $30^{\circ}$ , a significant (99% confidence level) correlation of 0.672 is obtained and nearly half (45%) of the true variance is explained by the observed extratropical atmosphere (Figures 1c). This demonstrates a significant impact of the extratropical atmosphere on the tropical Pacific interannual variability. When both ADA and ODA are activated poleward of  $30^{\circ}$ , the tropical Pacific SSTA remains almost the same as that in ada30 and no significant change occurs to the ACC and RMSE values. This implies that the extratropical SST poleward of  $30^{\circ}$  is not effective in generating the tropical Pacific variability (Figure 1d), which is consistent with previous studies [34], [47].

The addition of restoring walls into the ocean divides the extratropical impact into different pathways. When subPR walls are inserted, the oceanic teleconnections are cut-off at the corresponding latitudes; thus, only the atmospheric pathway and surface coupling are allowed to transfer the extratropical variability equatorward. When subPR walls are inserted between  $20^{\circ}$  and  $30^{\circ}$ , no significant impact is made on the tropical Pacific SSTA compared with ada30 (Figure 1e). This implies that the ocean poleward of  $20^{\circ}$  is ineffective in generating the tropical Pacific interannual variability. If surface coupling is further cut-off by colPR, the atmosphere is the only effective pathway to connect the tropical variability with extratropical forcing. The tropical Pacific variability is slightly worse reconstructed in colpr20 with decreased ACC of 0.639 and increased RMSE of 0.446 (Figure 1f), and less tropical Pacific variance can be explained. Recalling the ineffectiveness of subpr20, the change in colpr20 indicates a slight impact of surface coupling poleward of  $20^{\circ}$ . When subPR walls are moved equatorward till between  $10^{\circ}$  and  $20^{\circ}$ , the model also shows a poorer ability to reconstruct the truth in the tropical Pacific (Figure 1g). This indicates that the oceanic pathway is able to impact the tropical Pacific variability from a closer distance. If surface coupling is further cut-off, the model exhibits a significantly poorer reproduction ability (Figure 1h) with less than half (21%) of the explained variance in ada30. This implies a significant impact on the tropical Pacific variability is attributed to the surface coupling as closer to the equator.

The extratropical impact on the tropical Pacific can be more clearly and systematically examined in the coupled system of the Pacific region. Figure 2 shows the zonally averaged ACC of temperature in the coupled ocean-atmosphere system in the Pacific region. With no active ADA in any region, the ACC of ctrl is low both in the atmosphere and ocean (Figure 2a). When ADA is activated poleward of  $30^{\circ}$ , the ACC of the extratropical atmosphere is largely improved because of the continuous constraint of observations (Figure 2b). The improved extratropical atmosphere further benefits the atmosphere equatorward of  $30^{\circ}$  and the underlying ocean via atmospheric dynamics and ocean-atmosphere coupling interactions, respectively.

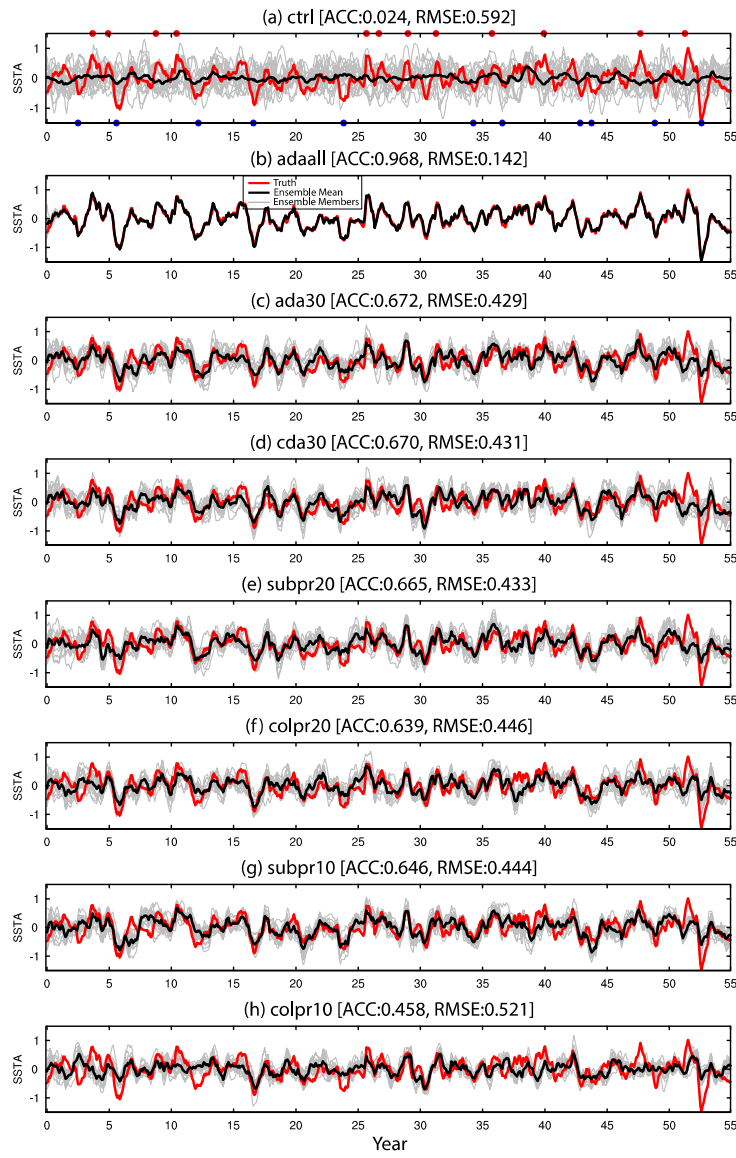


**FIGURE 1.** Time series of the area-averaged tropical Pacific SSTAs from (a) ctrl, (b) adaall, (c) ada30, (d) cda30, (e) subpr20, (f) colpr20, (g) subpr10, and (h) colpr10. Red lines indicate the truth, black lines the ensemble-mean, and grey lines all 16 ensemble members. Solid red (blue) circles in (a) indicate identified El Niño (La Niña) events in truth.

When subPR walls are inserted, the correlations within the restoring walls are significantly reduced, establishing two walls cutting-off the meridional oceanic connections in the subsurface ocean. When subPR walls are inserted between 20° and 30°, no significant impact is made on the tropical Pacific, especially at the surface (Figure 2c). This indicates the ineffectiveness of the ocean poleward of 20° in generating the tropical Pacific interannual variability. The ACC of the tropical Pacific shows a slight reduction at both the surface and subsurface when the subPR walls are placed between 10° and 20° (Figure 2e). Considering the ineffectiveness of subpr20 in affecting the tropical Pacific, this implies that the oceanic pathway plays a role at a closer distance to the equator. When colPR is adopted, the meridional

connections at corresponding restoring latitudes can only be accomplished through the atmospheric pathway; thus, the tropical Pacific variability is more poorly reproduced than in the corresponding subPR experiments (Figures 2d and 2f). Difference between corresponding subPR and colPR runs indicates the impact from surface coupling. Results show that surface coupling can affect the tropical Pacific variability from a further extratropical distance than the oceanic pathway with increasing impact as closer to the equator. More specifically, when the surface coupling between 10° and 20° is blocked in colpr10 (Figure 2f), the tropical Pacific variability is significantly impacted. Furthermore, the poor status of the tropical Pacific further deteriorates the overlying atmosphere through coupling dynamics.

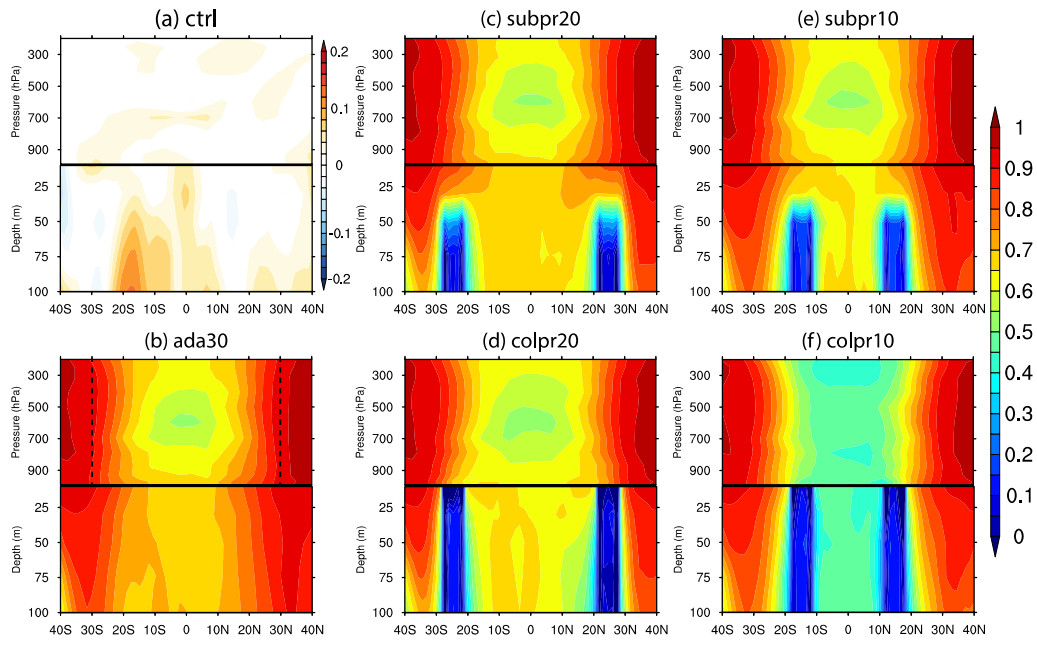


**FIGURE 2.** Zonally averaged ACC of atmosphere and ocean temperature in the Pacific region (120°E-70°W) between 40°S and 40°N. Dashed lines in (b) indicate the equator-side boundaries of ADA.

### B. QUANTIFYING ISOLATED EXTRATROPICAL CONTRIBUTION

The relative contributions of three pathways to the genesis of tropical Pacific interannual variability is isolated and quantitatively estimated based on ACC. The ACCs of the tropical Pacific SST are first squared to transform correlations to the explained variances. Then the relative contribution of each pathway is calculated at different latitudes as follows:

$$Atmos = ACC_{colpr}^2 / ACC_{ada}^2 \quad (3)$$

$$Ocean = (ACC_{ada}^2 - ACC_{subpr}^2) / ACC_{ada}^2 \quad (4)$$

$$Coupl = (ACC_{subpr}^2 - ACC_{colpr}^2) / ACC_{ada}^2 \quad (5)$$

where  $ACC_{ada}^2$  in the denominator indicates the total impact from the extratropical atmosphere poleward of 30°,  $ACC_{colpr}^2$  is the remaining impact from the atmosphere when the oceanic teleconnections and surface coupling are both cut-off by colPR,  $ACC_{ada}^2 - ACC_{subpr}^2$  is the reduction in the total when only the oceanic pathway is removed by subPR (i.e., the impact from the ocean), and  $ACC_{subpr}^2 - ACC_{colpr}^2$  is the remaining impact after the contributions from the atmosphere and the ocean are both subtracted from the total (i.e., the impact from surface coupling). Therefore, “Atmos”, “Ocean”, and “Coupl” in above equations indicate the individual relative contributions of the atmosphere, ocean, and surface coupling, respectively, in transferring the extratropical atmospheric variability equatorward. Here, we note that the total impact is computed as  $ACC_{ada}^2$ , rather than the squared difference between ada and ctrl. This is because the ctrl experiment assimilates no observations, and the ACC of its ensemble-mean is spuriously higher than the theoretical value of 0 but does not represent the physical variability.

Therefore, the theoretical ACC value of ctrl (i.e., 0) should be used in above calculations.

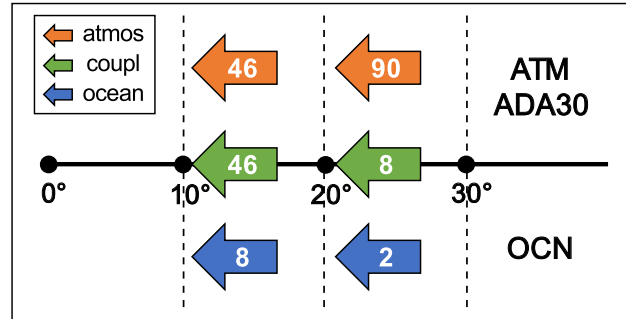


**FIGURE 3.** Extratropical percentage contributions of the atmosphere (orange), ocean (blue), and surface coupling (green) to the tropical Pacific interannual variability of SST at different latitudes.

Based on above calculations, Figure 3 shows a quantified schematic of how the extratropical atmosphere impacts the tropical Pacific interannual variability through three pathways. In all restoring experiments, ADA is only activated poleward of 30° and the ctrl experiment hardly explains any variance of the tropical Pacific. Thus, all the impact on the tropical Pacific variability originally comes from the observed extratropical atmosphere, which corresponds to the original total extratropical signal in this study. However, the partition of contributions among three types of teleconnections varies with latitude. Poleward of 20°, the extratropical impact is dominated by the atmospheric pathway, which is responsible for 90% of the total impact. At the same location, surface coupling only accounts for a small section (8%) of the extratropical influence,

while the oceanic pathway barely contributes none (2%). Towards the equator, less contribution is attributed to the atmosphere, while more to the surface coupling and the oceanic pathway. Poleward of  $10^{\circ}$ , the atmosphere no longer holds the dominant position for the tropical Pacific variability (from 90% to 46%), while the impact from surface coupling significantly increases (from 8% to 46%). Now the atmospheric pathway and surface coupling together play a dominant role (a sum of 92%) in the genesis of tropical Pacific variability. The significantly increased contribution of surface coupling as closer to the equator is consistent with previous studies [34], [47]. Although the impact from the oceanic pathway also increases as closer to the equator, its contribution is still very small (8%) poleward of  $10^{\circ}$ . The quantification based on RMSE is also conducted, and consistent results are obtained.

Generally, processes in the atmosphere have fast temporal and large spatial scales, therefore the atmospheric teleconnections can impact the tropical Pacific far from the equator (e.g., poleward of  $30^{\circ}$ ). While the oceanic processes have relatively slow temporal and small spatial scales, so the ocean only contributes to the tropical variability with a limited amount even at a close distance on the timescale considered here. We speculate that the oceanic teleconnections may affect the tropical climate from a further distance for the decadal timescale and beyond, such as through the coastal Kelvin wave at the western boundary [18] and the equatorward subduction [20], [21]. While for the interannual timescale considered here, maybe the influence of those teleconnections is too insignificant to be recognized. It should be noted that the oceanic contribution in this study does not represent the total impact from the extratropical ocean as in the real world. Because only the extratropical atmosphere is assimilated, the oceanic contribution here represents the impact of oceanic variabilities that can be generated by the extratropical atmospheric forcing. In addition, coupled ocean-atmosphere interactions usually have intermediate temporal and spatial scales in comparison with those in the atmosphere and ocean. Therefore, although surface coupling can impact the tropical Pacific from a relatively far distance, its contribution significantly amplifies at a close distance to the equator.

### C. NEAR-EQUATOR SURFACE COUPLING

The significant impact of the near-equator surface coupling on the tropical Pacific interannual variability is clearly shown in the seasonality of the tropical Pacific variability. Figure 4 shows the standard deviations of the tropical Pacific SSTA by calendar month. The maximum standard deviation in truth occurs in July, implying an early shift of ENSO in FOAM compared with in the real world. The seasonality of tropical Pacific variability in adaall is quite similar to that in truth, which shows the effectiveness of ADA across the globe in reconstructing the tropical Pacific variability. In contrast, when no ADA is activated anywhere, the variability in ctrl is reduced significantly in all months and

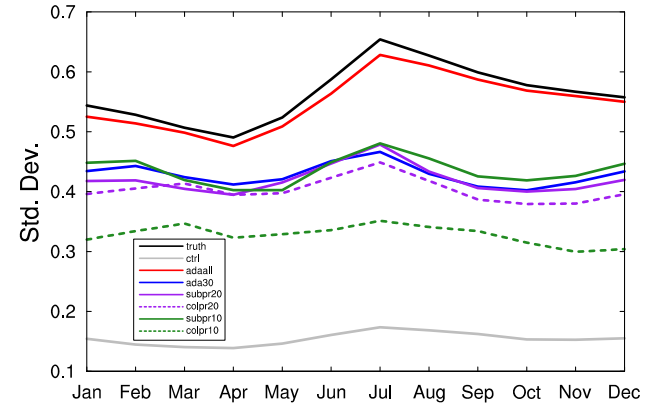


**FIGURE 4.** Standard deviations of tropical Pacific SSTA by calendar month.

no significant seasonal change exists. In ada30, the overall variability and seasonality are both similar to the truth, albeit smaller in magnitude for all months. This demonstrates the significant control of extratropical atmosphere on the tropical Pacific variability. In subpr20, colpr20, and subpr10, the tropical Pacific variabilities all stay close to that in ada30. When the coupling interactions between  $10^{\circ}$  and  $20^{\circ}$  are blocked in colpr10, the variability is significantly reduced with respect to ada30 in all months and the seasonality also disappears. This indicates a significant role of the near-equator coupling interactions, more specifically between  $10^{\circ}$  and  $20^{\circ}$ , in generating the tropical Pacific variability.

Near-equator surface coupling shows a significant role in generating the tropical Pacific interannual variability in above results. Now we explore the impact of the near-equator coupling interactions based on the composite of ENSO, the strongest interannual variability in the tropical Pacific. El Niño and La Niña events are identified from the truth using a Nino3.4 ( $5^{\circ}\text{S}$ - $5^{\circ}\text{N}$ ,  $120^{\circ}\text{W}$ - $170^{\circ}\text{W}$ ) index of  $1.0^{\circ}$  as the criterion. Here,  $1.0^{\circ}$  is selected because it indicates a variability magnitude very unlikely to be generated in the ensemble-mean anomaly by only the natural variability of FOAM, i.e., the ctrl run (Figure 1a). Therefore, the genesis of any ENSO event should be ultimately attributed to the observed extratropical atmosphere. The events are selected from the truth, instead of each experiment. Although each experiment generates their own events, the truth provides a unified standard for all experiments. Thus, an El Niño (La Niña) event is counted if the monthly Nino3.4 index in the truth exceeds the positive (negative)  $1.0^{\circ}$ . Considering that two identified events may exist very close to each other and the weak phase-locking of ENSO events, only the events that have peak values within one year but are more than 6 months apart are kept. The identified El Niño (La Niña) events in the truth are illustrated with solid red (blue) circles in Figure 1a. Similar to L17, we use the ctrl experiment as a benchmark to evaluate the significance of others. The distribution of the anomaly from ctrl specifies the magnitude of the natural

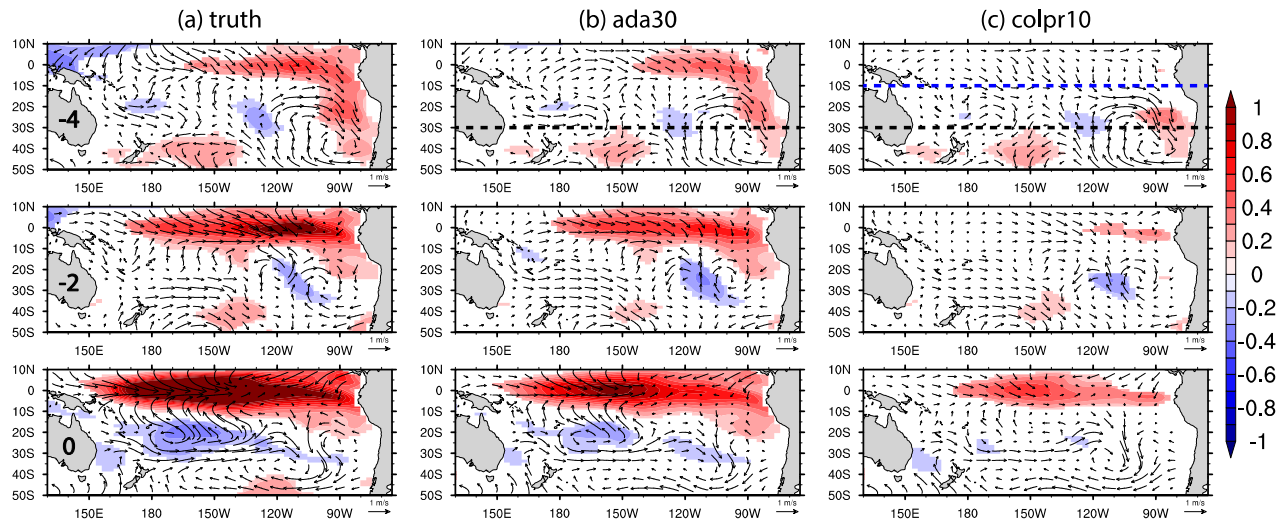


**FIGURE 5.** Composites of anomalous SST (shadings,  $^{\circ}$ ) and wind (arrows) at 4, 2, and 0 months prior to the peak of Niño3.4 in (a) truth, (b) ada30, and (c) colpr10. Numbers of months prior to the peak are marked in (a). SSTAs are only shown where they exceed CTRL\_SD. Dashed black (blue) lines in the first row indicate the equator-side boundaries of ADA (PR).

variability without any observational information. Therefore, the standard deviations of the ctrl anomaly (hereafter “CTRL\_SD”) can be used as a significance criterion.

Near-equator coupled interactions significantly affect the ENSO onset by modulating the PMM. Composites of SST and low-level wind anomalies in the South Pacific are shown in Figure 5 at 4, 2, and 0 months prior to the Niño3.4 peak (La Niña events are included with reversed sign). Here only the tropical and South Pacific are shown, because the North Pacific can be analyzed in a similar fashion. The SSTAs are visible only where they exceed CTRL\_SD (i.e., significant with respect to the ctrl variability). In the truth (Figure 5a), the extratropical variability propagates into the tropical Pacific via the SPMM [28]. At 4 months prior to the Niño3.4 peak, there are already positive SSTAs in the tropical eastern Pacific. In the meantime, the anomalous northwestlies in the subtropical southeastern Pacific reduce the climatological southeasterly trade winds. The underlying ocean is warmed because of the reduced latent heat flux out of the ocean due to reduced trade winds. The warm SSTAs would induce anomalous westerlies on the equator-side, which further reduce the climatological trade winds and latent heat flux there, allowing the coupled wind-SST anomalies to propagate equatorward. Two months later, the westerly anomalies persist in the subtropical southeastern Pacific, thus the reduced latent heat flux continues to warm the SST there. The warm SSTAs in the tropical eastern Pacific are intensified, with the subtropical warm center moving equatorward to approximately 20°S. As such, the coupled extratropical wind-SST anomalies propagate into the deep tropics. When the extratropical atmosphere poleward of 30°S is assimilated in ada30 (Figure 5b), the wind anomalies poleward of 30°S are continuously corrected by the observations, thus quite similar to the truth. The extratropical atmosphere impacts the tropical variability through a similar coupled anomalous wind-SST process as in truth with reduced magnitude both

prior to and at the Niño3.4 peak. The wind anomalies extending equatorward of 30°S, where no assimilation is activated, could be caused by the atmospheric dynamic adjustment [8]. In subpr20, colpr20, and subpr10, the equatorward propagation of the coupled wind-SST anomalies is similar to that in ada30 with similar magnitude of tropical Pacific SSTAs at the Niño3.4 peak (not shown). The coupled interactions between 10°S and 20°S, however, can significantly impact the coupled equatorward propagation process and subsequently the genesis of ENSO. When the coupled interactions between 10°S and 20°S are blocked in colpr10 (Figure 5c), the pre-existing warm SSTAs in the tropical eastern Pacific are almost invisible. Although there exist coupled westerly and warm SST anomalies in the subtropical southeastern Pacific at 4 months prior to the Niño3.4 peak, the suppression of the surface coupling between 10°S and 20°S prevents the coupled anomalies from further propagating equatorward. As a result, the ENSO variability is very poorly reproduced at the Niño3.4 peak.

Near-equator surface coupling significantly impacts the ENSO onset by facilitating the preconditioning of the equatorial Pacific heat content. Composites of meridionally averaged equatorial (3°S-3°N) Pacific upper ocean temperature anomalies at 12, 6, and 0 months prior to the Niño3.4 peak are shown in Figure 6. Before ENSO onset, a subsurface warming develops in the equatorial western Pacific, growing in magnitude and propagating upward and eastward to the surface equatorial eastern Pacific (Figure 6a). In the truth, a significant warming exists in the subsurface equatorial western Pacific at 12 months prior to the Niño3.4 peak. This subsurface warming develops in magnitude with time and propagates upward and eastward along the thermocline. 6 months later, the intensified subsurface warming has already arrived at the surface eastern Pacific and almost expands in the entire equatorial upper Pacific. At the Niño3.4 peak, significant warming anomalies

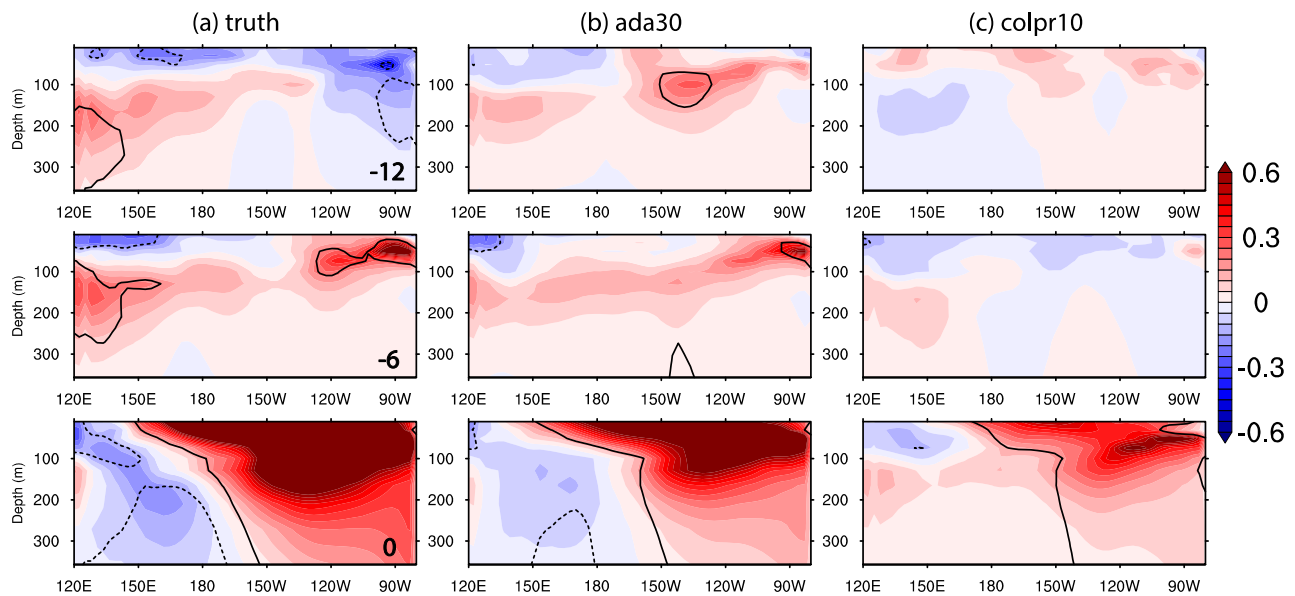


**FIGURE 6.** Composites of meridionally averaged equatorial Pacific ( $3^{\circ}\text{S}$ - $3^{\circ}\text{N}$ ) anomalous upper ocean temperature at 12, 6, and 0 months prior to the peak of Niño3.4 in (a) truth, (b) ada30, and (c) colpr10. Numbers of months prior to the peak are marked in (a). Solid (dashed) contours indicate ratios of positive (negative) one of the composite anomalies to CTRL\_SD.

are located in the equatorial central and eastern upper Pacific. Meanwhile, a weak subsurface cooling develops in the subsurface western Pacific. This equatorial oceanic process illustrated in Figure 6a is consistent with the classical delayed recharge oscillator theory of ENSO [48], [49]. In ada30, albeit smaller in magnitude, the upward and eastward propagation of the subsurface warming in the western Pacific can be similarly reconstructed both in magnitude and timing (Figure 6b), which implies a significant impact of the extratropical atmosphere on the preconditioning of the equatorial Pacific heat content. In subpr20, colpr20, and subpr10, the propagation of heat content is also similarly reproduced as in ada30 (not shown). However, colpr10 fails to reproduce this process (Figure 6c). At 12 and 6 months prior to the Niño3.4 peak, almost no significant warming can be recognized in the entire equatorial upper Pacific. As a result, the central and eastern warming in the equatorial upper Pacific at the Niño3.4 peak is greatly reduced in magnitude. This demonstrates a significant impact of the near-equator coupling interactions in the preconditioning of the equatorial Pacific heat content. The significant suppression of the equatorial upper Pacific warming in colpr10 may be caused by the suppression of the westerly anomalies in the tropical Pacific both prior to and at the Niño3.4 peak by the blocking of the near-equator coupling interactions. In the absence of coupling interactions between  $10^{\circ}$  and  $20^{\circ}$ , westerly anomalies are poorly reconstructed and largely reduced in magnitude in the tropical Pacific.

#### IV. SUMMARY AND CONCLUSION

In this study, the extratropical atmospheric impact on the tropical Pacific interannual variability is quantitatively divided into three pathways at different latitudes in a CGCM,

aided by two modeling techniques: RCDA and PR. Our study represents a more comprehensive attempt to quantify the extratropical impact on the tropical Pacific variability than the recent studies by Amaya *et al.* [47] and Liguori and Di Lorenzo [50]. To the best of our knowledge, this is the first study to quantitatively isolate the extratropical impact on tropical variability into three types of teleconnections in a fully coupled system. The sole use of ADA of the CDA system in the extratropical atmosphere guarantees that the extratropical atmosphere is the only source of observational information to generate the tropical Pacific variability. The colPR and subPR approaches are further used to separate three pathways by inserting restoring walls into the ocean component of the coupled system at desired latitude bands. The use of ensemble averaging filters out the tropical variability that is generated by only the model natural variability in each member. The joint use of RCDA, colPR, and subPR enables the isolation of individual contributions of atmospheric, oceanic, and coupled ocean-atmosphere teleconnections in transferring the extratropical atmospheric variability equatorward.

The joint analysis of various experiments provides us with a quantified schematic showing how the extratropical atmosphere affects the tropical Pacific interannual variability via three types of teleconnections as progressively closer to the equator. For the timescale considered here, all signals originate from the atmosphere poleward of  $30^{\circ}$ . Poleward of  $20^{\circ}$ , the extratropical impact is dominated by the atmospheric pathway, which is responsible for 90% of the total contribution. As closer to the equator, less impact is contributed by the atmospheric teleconnections, while more is attributed to the coupled teleconnections and the oceanic pathway. Poleward of  $10^{\circ}$ , 46% of the total impact

comes from the atmosphere, while the contribution from the surface coupling significantly increases from 8% to 46%. Although the contribution from the oceanic pathway also increases as closer to the equator, the ocean only accounts for 8% of the total extratropical impact poleward of 10°. Due to the differences in temporal and spatial scales in different components, the atmosphere can impact the tropical Pacific far from the equator, while the ocean only has a limited influence even at a close distance to the equator. Lying between scales of the atmosphere and ocean, coupled ocean-atmosphere teleconnections are able to affect the tropical Pacific from a further distance than the ocean, but the impact only significantly amplifies at a close distance to the equator. To explore the significant role of the near-equator surface coupling in impacting the tropical Pacific variability, composite analyses of ENSO events are conducted. Results show that the near-equator coupled interactions significantly impact the onset of ENSO by modulating the PMM and the preconditioning of equatorial Pacific heat content. It is also necessary to point out that the latitude boundaries for both RCDA and PR in this study are approximations for different regions and may not be strictly applicable to other models or the real world.

There are still many related issues to be further explored. In this paper, the extratropical impact on tropical variability is only estimated for different latitudes in both hemispheres. Liguori and Di Lorenzo [50] suggested that the impact of each hemisphere could be different. The contribution from each hemisphere can be further explored. In addition, given the relatively short time period of our experiments, only the interannual variability of the tropical Pacific is considered in this study. Longer simulations can be performed to explore the extratropical impact on tropical variability at longer timescales (e.g., decadal or multidecadal) to obtain a more complete schematic across different timescales. As a pilot study, the main purpose of this study is to isolate and quantify the individual relative contributions of three types of teleconnections. The mechanisms for the extratropics-tropics interactions need to be further explored in the future. For example, the dominant role of the atmospheric teleconnections poleward of 20° proposes another interesting question for the extratropics-tropics interactions, which needs to focus on the atmospheric physical processes with more targeted experiment design. The study here is also desired to be repeated in other popular and state-of-the-art CGCMs.

## ACKNOWLEDGMENT

The authors acknowledge high-performance computing support from Cheyenne of NCAR's CISL.

## REFERENCES

- [1] Z. Liu and M. Alexander, "Atmospheric bridge, oceanic tunnel, and global climatic teleconnections," *Rev. Geophys.*, vol. 45, no. 2, pp. 1–34, 2007.
- [2] N. J. Mantua, S. R. Hare, Y. Zhang, J. M. Wallace, and R. C. Francis, "A Pacific interdecadal climate oscillation with impacts on salmon production," *Bull. Amer. Meteorol. Soc.*, vol. 78, no. 6, pp. 1069–1080, Jun. 1997.
- [3] Y. Zhang, J. M. Wallace, and D. S. Battisti, "ENSO-like interdecadal variability: 1900–93," *J. Climate*, vol. 10, no. 5, pp. 1004–1020, May 1997.
- [4] N.-C. Lau and M. J. Nath, "The role of the 'atmospheric bridge' in linking tropical pacific ENSO events to extratropical SST anomalies," *J. Climate*, vol. 9, no. 9, pp. 2036–2057, Sep. 1996.
- [5] S. A. Klein, B. J. Soden, and N.-C. Lau, "Remote sea surface temperature variations during ENSO: Evidence for a tropical atmospheric bridge," *J. Climate*, vol. 12, no. 4, pp. 917–932, Apr. 1999.
- [6] M. A. Alexander, I. Bladé, M. Newman, J. R. Lanzante, N.-C. Lau, and J. D. Scott, "The atmospheric bridge: The influence of ENSO teleconnections on air-sea interaction over the global oceans," *J. Climate*, vol. 15, no. 16, pp. 2205–2231, Aug. 2002.
- [7] T. P. Barnett, D. W. Pierce, M. Latif, D. Dommenget, and R. Saravanan, "Interdecadal interactions between the tropics and midlatitudes in the pacific basin," *Geophys. Res. Lett.*, vol. 26, no. 5, pp. 615–618, Mar. 1999.
- [8] D. W. Pierce, T. P. Barnett, and M. Latif, "Connections between the pacific ocean tropics and midlatitudes on decadal timescales," *J. Climate*, vol. 13, no. 6, pp. 1173–1194, Mar. 2000.
- [9] P. J. Webster and J. R. Holton, "Cross-equatorial response to middle-latitude forcing in a zonally varying basic state," *J. Atmos. Sci.*, vol. 39, no. 4, pp. 722–733, Apr. 1982.
- [10] C. Deser, J. E. Walsh, and M. S. Timlin, "Arctic sea ice variability in the context of recent atmospheric circulation trends," *J. Climate*, vol. 13, no. 3, pp. 617–633, Feb. 2000.
- [11] J. C. H. Chiang and C. M. Bitz, "Influence of high latitude ice cover on the marine intertropical convergence zone," *Climate Dyn.*, vol. 25, no. 5, pp. 477–496, Oct. 2005.
- [12] M. Nonaka and S. P. Xie, "Propagation of North Pacific interdecadal subsurface temperature anomalies in an ocean GCM," *Geophys. Res. Lett.*, vol. 27, no. 22, pp. 3747–3750, 2000.
- [13] S.-I. Shin and Z. Liu, "Response of the equatorial thermocline to extratropical buoyancy forcing," *J. Phys. Oceanogr.*, vol. 30, no. 11, pp. 2883–2905, Nov. 2000.
- [14] Z. Liu, S.-I. Shin, B. Otto-Bliesner, J. E. Kutzbach, E. C. Brady, and D. Lee, "Tropical cooling at the last glacial maximum and extratropical ocean ventilation," *Geophys. Res. Lett.*, vol. 29, no. 10, pp. 481–484, 2002.
- [15] Z. Liu and H. Yang, "Extratropical control of tropical climate, the atmospheric bridge and oceanic tunnel," *Geophys. Res. Lett.*, vol. 30, no. 5, pp. 341–344, Mar. 2003.
- [16] M. Kawase, "Establishment of deep ocean circulation driven by deep-water production," *J. Phys. Oceanogr.*, vol. 17, no. 12, pp. 2294–2317, Dec. 1987.
- [17] H. L. Johnson and D. P. Marshall, "A theory for the surface Atlantic response to thermohaline variability," *J. Phys. Oceanogr.*, vol. 32, no. 4, pp. 1121–1132, Apr. 2002.
- [18] J. Lysne, P. Chang, and B. Giese, "Impact of the extratropical pacific on equatorial variability," *Geophys. Res. Lett.*, vol. 24, no. 21, pp. 2589–2592, Nov. 1997.
- [19] J. Yang, "A linkage between decadal climate variations in the labrador sea and the tropical Atlantic Ocean," *Geophys. Res. Lett.*, vol. 26, no. 8, pp. 1023–1026, Apr. 1999.
- [20] Z. Liu, S. G. H. Philander, and R. C. Pacanowski, "A GCM study of tropical–subtropical upper-ocean water exchange," *J. Phys. Oceanogr.*, vol. 24, no. 12, pp. 2606–2623, Dec. 1994.
- [21] B. Huang and Z. Liu, "Pacific subtropical-tropical thermocline water exchange in the national centers for environmental prediction ocean model," *J. Geophys. Res., Oceans*, vol. 104, no. C5, pp. 11065–11076, May 1999.
- [22] Z. Liu and S. Xie, "Equatorward propagation of coupled air-sea disturbances with application to the annual cycle of the Eastern Tropical Pacific," *J. Atmos. Sci.*, vol. 51, no. 24, pp. 3807–3822, Dec. 1994.
- [23] D. J. Vimont, D. S. Battisti, and A. C. Hirst, "Footprinting: A seasonal connection between the tropics and mid-latitudes," *Geophys. Res. Lett.*, vol. 28, no. 20, pp. 3923–3926, Oct. 2001.
- [24] D. J. Vimont, D. S. Battisti, and A. C. Hirst, "The seasonal footprinting mechanism in the CSIRO general circulation models," *J. Climate*, vol. 16, no. 16, pp. 2653–2667, Aug. 2003.
- [25] D. J. Vimont, J. M. Wallace, and D. S. Battisti, "The seasonal footprinting mechanism in the Pacific: Implications for ENSO," *J. Clim.*, vol. 16, no. 16, pp. 2668–2675, 2003.
- [26] J. C. H. Chiang and D. J. Vimont, "Analogous pacific and Atlantic meridional modes of tropical atmosphere–ocean Variability," *J. Climate*, vol. 17, no. 21, pp. 4143–4158, Nov. 2004.

- [27] P. Chang, L. Zhang, R. Saravanan, D. J. Vimont, J. C. H. Chiang, L. Ji, H. Seidel, and M. K. Tippett, "Pacific meridional mode and el Niño-southern oscillation," *Geophys. Res. Lett.*, vol. 34, no. 16, pp. 1–5, Aug. 2007.
- [28] H. Zhang, A. Clement, and P. Di Nezio, "The south pacific meridional mode: A mechanism for ENSO-like variability," *J. Climate*, vol. 27, no. 2, pp. 769–783, Jan. 2014.
- [29] R. Ding, J. Li, Y.-H. Tseng, C. Sun, and F. Xie, "Joint impact of North and South Pacific extratropical atmospheric variability on the onset of ENSO events," *J. Geophys. Res., Atmos.*, vol. 122, no. 1, pp. 279–298, Jan. 2017.
- [30] A. Czaja, P. van der Vaart, and J. Marshall, "A diagnostic study of the role of remote forcing in tropical Atlantic variability," *J. Climate*, vol. 15, no. 22, pp. 3280–3290, Nov. 2002.
- [31] S.-P. Xie and Y. Tanimoto, "A pan-Atlantic decadal climate oscillation," *Geophys. Res. Lett.*, vol. 25, no. 12, pp. 2185–2188, Jun. 1998.
- [32] L. Wu, D. E. Lee, and Z. Liu, "The 1976/77 North Pacific climate regime shift: The role of subtropical ocean adjustment and coupled ocean-atmosphere feedbacks," *J. Climate*, vol. 18, no. 23, pp. 5125–5140, Dec. 2005.
- [33] L. Wu, Z. Liu, C. Li, and Y. Sun, "Extratropical control of recent tropical Pacific decadal climate variability: A relay teleconnection," *Climate Dyn.*, vol. 28, no. 1, pp. 99–112, Nov. 2006.
- [34] F. Lu, Z. Liu, Y. Liu, S. Zhang, and R. Jacob, "Understanding the control of extratropical atmospheric variability on ENSO using a coupled data assimilation approach," *Climate Dyn.*, vol. 48, nos. 9–10, pp. 3139–3160, May 2017.
- [35] R. Jacob, C. Schafer, I. Foster, and E. Al, "Computational design and performance of the fast ocean atmosphere model, version one," in *Proc. Comput. Sci.*, 2001, pp. 175–184.
- [36] Y. Liu, Z. Liu, S. Zhang, X. Rong, R. Jacob, S. Wu, and F. Lu, "Ensemble-based parameter estimation in a coupled GCM using the adaptive spatial average method," *J. Climate*, vol. 27, no. 11, pp. 4002–4014, Jun. 2014.
- [37] Y. Liu, Z. Liu, S. Zhang, R. Jacob, F. Lu, X. Rong, and S. Wu, "Ensemble-based parameter estimation in a coupled general circulation model," *J. Climate*, vol. 27, no. 18, pp. 7151–7162, Sep. 2014.
- [38] F. Lu, Z. Liu, S. Zhang, Y. Liu, and R. Jacob, "Strongly coupled data assimilation using leading averaged coupled covariance (LACC). Part II: CGCM experiments," *Monthly Weather Rev.*, vol. 143, no. 11, pp. 4645–4659, Nov. 2015.
- [39] F. Lu, Z. Liu, S. Zhang, and R. Jacob, "Assessing extratropical impact on the tropical bias in coupled climate model with regional coupled data assimilation," *Geophys. Res. Lett.*, vol. 44, no. 7, pp. 3384–3392, Apr. 2017.
- [40] F. Lu and Z. Liu, "Assessing extratropical influence on observed El Niño-Southern oscillation events using regional coupled data assimilation," *J. Clim.*, vol. 31, no. 21, pp. 8961–8969, 2018.
- [41] J. L. Anderson, "An ensemble adjustment Kalman filter for data assimilation," *Monthly Weather Rev.*, vol. 129, no. 12, pp. 2884–2903, Dec. 2001.
- [42] J. L. Anderson, "A local least squares framework for ensemble filtering," *Monthly Weather Rev.*, vol. 131, no. 4, pp. 634–642, Apr. 2003.
- [43] S. Zhang, M. J. Harrison, A. Rosati, and A. Wittenberg, "System design and evaluation of coupled ensemble data assimilation for global oceanic climate studies," *Monthly Weather Rev.*, vol. 135, no. 10, pp. 3541–3564, Oct. 2007.
- [44] Z. Liu, L. Wu, R. Gallimore, and R. Jacob, "Search for the origins of Pacific decadal climate variability," *Geophys. Res. Lett.*, vol. 29, no. 10, pp. 42-1–42-4, 2002.
- [45] L. Wu, "Is tropical Atlantic variability driven by the North Atlantic oscillation?" *Geophys. Res. Lett.*, vol. 29, no. 13, pp. 31–34, 2002.
- [46] L. Wu, Z. Liu, R. Gallimore, R. Jacob, D. Lee, and Y. Zhong, "Pacific decadal variability: The tropical pacific mode and the North Pacific mode," *J. Climate*, vol. 16, no. 8, pp. 1101–1120, Apr. 2003.
- [47] D. J. Amaya, Y. Kosaka, W. Zhou, Y. Zhang, S.-P. Xie, and A. J. Miller, "The North Pacific pacemaker effect on historical ENSO and its mechanisms," *J. Climate*, vol. 32, no. 22, pp. 7643–7661, Nov. 2019.
- [48] M. A. Cane and S. E. Zebiak, "A theory for El Niño and the Southern oscillation," *Science*, vol. 228, no. 4703, pp. 1085–1087, May 1985.
- [49] F.-F. Jin, "An equatorial ocean recharge paradigm for ENSO. Part I: Conceptual model," *J. Atmos. Sci.*, vol. 54, no. 7, pp. 811–829, Apr. 1997.
- [50] G. Liguori and E. Di Lorenzo, "Separating the north and south pacific meridional modes contributions to ENSO and tropical decadal variability," *Geophys. Res. Lett.*, vol. 46, no. 2, pp. 906–915, Jan. 2019.



**JINGZHE SUN** received the M.S. degree in computer science and technology from the National University of Defense Technology, Changsha, China, in 2015, where he is currently pursuing the Ph.D. degree in computer science and technology. His main research interests include coupled data assimilation and coupled ocean-atmosphere system modeling.



**ZHENGYU LIU** received the Ph.D. degree in physical oceanography from the Massachusetts Institute of Technology, Cambridge, MA, USA, in 1991. He is currently the Max Thomas Professor with The Ohio State University, Columbus, OH, USA. His research interests include ocean-atmosphere-land interaction and climate dynamics, dynamics of oceanic circulation, and Earth system modeling.



**FEIYU LU** received the Ph.D. degree in atmospheric and oceanic sciences from the University of Wisconsin–Madison, Madison, WI, USA, in 2017. He is currently a Postdoctoral Research Associate with Princeton University and NOAA/GFDL, Princeton, NJ, USA. His research interests include coupled data assimilation, climate variability, and climate prediction.



**WEIMIN ZHANG** received the Ph.D. degree in computer science and technology from the National University of Defense Technology, Changsha, China, in 2006. He is currently a Professor with the National University of Defense Technology. His research interests include data assimilation, numerical weather prediction, and Earth system modeling.



**YUCHU ZHAO** received the Ph.D. degree in atmospheric and oceanic sciences from Peking University, Beijing, China, in 2020. His research interests include data assimilation and ENSO variability.



**SHAOQING ZHANG** received the Ph.D. degree in meteorology from Florida State University, Tallahassee, FL, USA, in 2000. He is currently a Senior Professor with the Ocean University of China and the Qingdao National Laboratory of Marine Science and Technology. His research interests include data assimilation, Earth system modeling, and climate analysis and forecast.